NASA Technical Paper 2698

March 1987

Gear Tooth Stress Measurements on the UH-60A Helicopter Transmission

Fred B. Oswald

NASA

NASA
Technical
Paper
2698

1987

Gear Tooth Stress Measurements on the UH-60A Helicopter Transmission

Fred B. Oswald

Lewis Research Center
Cleveland, Ohio

NASA
National Aeronautics
and Space Administration

**Scientific and Technical
Information Branch**

Summary

The U.S. Army UH-60A (Black Hawk) 2200-kW (3000-hp) class twin-engine helicopter transmission was tested at the NASA Lewis Research Center. Results from these experimental (strain-gage) stress tests will enhance the data base for gear stress levels in transmissions of a similar power level. Strain-gage measurements were performed on the transmission's spiral-bevel combining pinions, the planetary sun gear, and ring gear. Tests were performed at rated speed and at torque levels 25 to 100 percent that of rated. One measurement series was also taken at a 90 percent speed level.

The largest stress found was 760 MPa (110 ksi) on the combining pinion fillet. This is 230 percent greater than the AGMA index stress. Corresponding mean and alternating stresses were 330 and 430 MPa (48 and 62 ksi). These values are within the range of successful test experience reported for other transmissions. On the fillet of the ring gear, the largest stress found was 410 MPa (59 ksi). The ring-gear peak stress was found to be 11 percent less than an analytical (computer simulation) value and it is 24 percent greater than the AGMA index stress. A peak compressive stress of 650 MPa (94 ksi) was found at the center of the tooth root of the sun gear.

Introduction

Helicopter transmission designers are continually striving for improvements in transmission life, reliability, and weight to power ratio. To accomplish these ends, designers must accurately predict stress levels in transmission components under realistic operating conditions. Prediction of gear stress presents a particular problem because of the geometry, complex and time-varying load sharing, and dynamic loading. There have been numerous reports of analytical and experimental stress-strain studies on external spur and helical gears (refs. 1 to 6). Not as much work has been performed on planetary transmissions (refs. 7 to 10) or on spiral-bevel gears (refs. 11 to 14).

This work was conducted to provide experimental strain-gage data for three of the component gears in the UH-60A Blackhawk helicopter transmission. These component gears are the sun gear, ring gear, and (spiral bevel) combining pinions. Results are presented in the form of time domain (during gear rotation) traces of measured stress, peak stress compared to location across gear face, and alternating stress compared to torque level. A table of summary results presents peak, mean, and alternating stress levels. The ring-gear peak stress result is compared to analytical (computer simulation) data (ref. 9).

Apparatus

Test Transmission

The UH-60A helicopter transmission has a twin (T700) engine power rating of 2109 kW (2828 hp). It provides 81.042:1 total speed reduction in three stages from the engine inputs (20909 rpm) to rotor output (258 rpm). There is also a tail shaft output (4117 rpm).

The transmission (figs. 1 and 2) consists of two input modules and one main module. The input modules contain the first reduction stage, a 22-tooth spiral-bevel input pinion driving an 80-tooth gear. The gear rotates with an internal overrunning ramp-roller clutch which drives a shaft leading to the main module of the transmission. The second reduction stage of the transmission (which combines the twin inputs) consists of two 17-tooth spiral-bevel pinions which drive a single 81-tooth combining gear. This gear is splined to a 62-tooth sun gear, the input to a planetary stage (third reduction). The sun gear drives five 83-tooth planet gears which revolve with their carrier within the stationary 228-tooth ring gear. The helicopter main rotor is driven directly from the planetary carrier. Tail rotor power is taken from a 116-tooth spiral bevel gear (on the back side of the combining gear) which drives a 34-tooth pinion. Total main rotor speed reduction is

$$\left(\frac{80}{22}\right)\left(\frac{81}{17}\right)\left(1+\frac{228}{62}\right)=81.042$$

Shaft speeds, gear tooth numbers, and gear vibration frequencies are shown in table I. Data for the instrumented (strain-gaged) gears is shown in table II.

Test Facility and Instrumentation

The NASA Lewis 2200 kW (3000 hp) Helicopter Transmission Test Facility (fig. 3) is a recirculating power (four-square) type. Power to the test transmission flows through two inputs (simulating two engines) and two outputs

(main rotor and tail drive). Power is provided by a constant-speed 600-kW induction motor. Since power flow is recirculating, only frictional losses need be replenished by the motor. Speed control is provided by an eddy current clutch. Torque (and hence circulating power) is induced independently in each loop by planetary torque units. The test facility is more fully described in references 15 and 16.

Strain gages were general-purpose electrical resistance constantan foil type having a gage length of 0.38 mm (0.015 in.). Strain gage signals from rotating gears were fed out through three slip-ring assemblies. One slip ring was on each of the two input modules (transmitting data from the combining spiral-bevel pinions) and an internal slip ring (mounted inside the main module above the combining bevel gear) transmitted data from the sun gear.

Procedure

A total of 50 strain gages were installed on the teeth of the sun, ring, and both right and left combining spiral-bevel pinions. To measure maximum tooth bending stresses, fillet gages were placed at the 30° tangency location (fig. 4) on the loaded side of the tooth fillet as per references 6 and 11. To measure rim bending stresses, root gages were placed in the center of the tooth root. Each instrumented tooth had five gages spaced evenly across the face width. On the sun gear, one tooth was instrumented with root gages. On the ring gear and both combining pinions, two consecutive teeth were instrumented with fillet gages and one tooth was instrumented with root gages. All gages were mounted along the plane normal to the tooth surface. Biaxial stress effects were neglected. The value used for Young's modulus is 203 GN/m^2 (203×10^3 MPa).

Strain gage readings were taken with constant-current dynamic strain-gage amplifiers. The signal from the strain amplifiers was stored on 14-channel FM tape for later analysis with an analog to digital converter (ADC) and a microcomputer. A five range T-bar switch was used to allow the recording of 50 strain gage signals on a single 14-channel tape. The strain gage measurement system is schematically shown in figure 5. Signals were low-pass filtered to reduce slip-ring noise. Filter cutoff frequencies (table II) were chosen to be at least 10 percent above the lowest frequency which caused a visible change in the stress waveform.

For each strain gage at each test condition, maximum and minimum stresses were averaged from several revolutions of the instrumented gear. The BASIC computer program GSG (Gear Strain Gage, LEW 14402) which was developed and used to reduce strain-gage data, search for maximum and minimum stresses, and plot stress waveforms is available from COSMIC. (Contact COSMIC, the University of Georgia, Athens, GA 30602, concerning the availability of this program.)

Data were acquired at 100 percent of rated speed and at torque levels of 25, 50, 75, and 100 percent of rated. To investigate possible speed effects, one additional series of readings were taken at 90 percent speed and 100 percent torque. Readings were not taken below 90 percent speed because of concerns of oil fouling the internal slip ring if rotating speed was not sufficient for oil "fling off". Throughout testing, the tail torque was maintained such that 16 percent of the input power flowed through the tail drive loop.

TABLE I.—SHAFT SPEEDS AND FREQUENCIES OF UH-60A TRANSMISSION AT 100 PERCENT ROTOR SPEED (258 rpm)

Gear Component	Number of teeth	Shaft speed, rpm	Shaft frequency, Hz
Spiral-bevel input pinion	22	20 909	348.5
Spiral-bevel input gear	80	5 750	95.83
Combining bevel pinion	17	5 750	95.83
Main bevel gear (lower)	81	1 207	20.11
Sun gear	62	1 207	[a]15.81
Planet gears (five)	83	451	[a]11.81
Carrier (output)	---	258	4.30
Ring gear	228	0	[a]4.30
Main bevel gear (upper)	116	1 207	20.11
Tail output gear	34	4 117	68.62

[a]Shaft frequencies for sun, planet, and ring gear are given relative to the carrier.

TABLE II.—DATA FOR INSTRUMENTED GEARS

	Combining pinion	Planetary ring gear	Planetary sun gear
Number of teeth	17	228	62
Teeth on mating gear(s)	81	83	83
Pitch circle diameter, mm	102.6	653.9	177.8
Face width, mm	65.0	60.5	81.5
Normal pressure angle, deg	20.0	22.5	22.5
Module, mm	6.04	2.87	2.87
Shaft angle, deg	81.8	0	0
Mean spiral angle, deg	25.0	-----	-----
Nominal (100 percent) torque, Nm	1750	51 600	14 000
Rotation speed (nominal), rpm	5750	0	1 207
Mesh frequency (100 percent speed), Hz	1629	980	980
Low pass filter frequency, Hz	1800	1 200	1 200

Results and Discussion

Experimental data in the form of stress traces is shown in figures 6 to 8. Stress is plotted against gear rotational position. On all traces, 0° is taken to be the location of maximum tensile stress. For the pinions, one full revolution (−180° to +180°) is shown. For the sun and ring gears, one planet pass (−36° to +36°) is shown. Since no notable differences in stress values were observed between the 90 and 100 percent speed readings, only 100 percent speed data is shown in this report.

Spiral-Bevel Combining Pinions

Typical stress traces at five locations across the face width of the spiral-bevel combining pinions during one revolution are shown in figure 6. Data from 10 revolutions of the gear have been averaged in this figure. Stress traces have been superimposed to show stress variation across the face width. Phase differences between traces are due to the stress distribution sweeping across the curved tooth surface as the gear rotates.

The stress waveforms (fig. 6) show a prominent compressive stress peak which occurs as the tooth preceding the instrumented tooth enters mesh. This is followed by a sharp tensile stress peak as the instrumented tooth is engaged. A small tensile plateau appears as the following tooth enters mesh. Secondary effects (such as gear rim deflection and the moving tangential stress as the the gear rotates) cause minor fluctuations in the stress traces.

As expected, fillet gages show much higher tensile stress levels as a result of tooth bending, while the root gages show more compressive stress from bending of the gear rim under the teeth. The stress distribution is shifted towards the heel end of the tooth, especially at higher torque levels.

Ring Gear

Ring gear stress is shown in figure 7. Figure 7(a) shows 10 planet passes (two carrier revolutions) to show repeatability of the data. No prominent differences between planets are seen. Figure 7(b) shows fillet gage stress and 7(c) shows root gage stress for one planet pass. In the ring gear, compressive stresses are much larger than in the combining pinions because of the flexibility of the thin gear body. (See ref. 4 for a discussion of backup ratio effects.) Since the ring gear is a reaction gear, the tensile stress peak precedes the compressive peak. Otherwise, the trace is similar to that of the combining pinions. Minor fluctuations along the trace are due to other teeth going through mesh (45.6 teeth per planet pass).

In figure 7(d), an analytical simulation of ring-gear tooth bending stress produced by the computer program GRDYMLT (refs. 7 to 9) is superimposed on experimental data from figure 7(b). In the analytical model, gear teeth are represented as linear springs connecting rigid gear bodies. (A new version of GRDYMLT, not yet available when the analytical study was performed, includes flexible ring gear and flexible carrier options.) Damping from tooth friction and from the oil film is modeled as a constant damping ratio. The damping ratio chosen here is 0.02 (2 percent). Structural damping (damping within the body of the gears) is not modeled.

Two obvious differences between the traces in figure 7(d) are as follows: (1) High frequency oscillations in the analytical trace do not appear in the experimental data and (2) the compressive stress of the experimental data does not appear in the analytical trace. The model had a higher frequency response than the actual transmission because the chosen damping ratio (2 percent) was fairly low and structural damping was not included. Since the ring gear was modeled as a rigid body, the compressive stress caused by bending of the ring gear body did not occur in the analytical simulation. Despite these differences, the analytical simulation is believed to model tooth bending stress (but not gear rim bending) reasonably well if the damping ratio is properly chosen.

Sun Gear

Sun gear root stress is shown in figure 8. Figure 8(a) shows 10 planet passes (two carrier revolutions) to show repeatability of the data. No prominent differences between planets are seen. Figure 8(b) shows an averaged root stress cycle (from 10 planet passes). The large compressive stress is the dominant feature in figure 8(b). This stress is due to gear rim inward bending (as a result of planet pass) added to a compressive hoop stress caused by the radial forces of all five planets. (On the ring gear, the compressive ring bending stress is partly offset by a tensile hoop stress.)

Figure 8 also shows slip ring noise. For this trace, data was filtered at 20 kHz (for anti-aliasing) rather than at the 1200 Hz used for maximum and minimum stress measurements. During a single planet pass, 12.4 tooth meshes will occur. Since the sun gear is relatively flexible (thin-rimmed), stress ripples from all 12 meshes are visible in figure 8(b).

No comparison between sun gear stress measurements and analytical simulation was made because GRDYMLT modeled tooth bending (fillet) stress rather than the root stress which was measured on the sun gear.

Figures 9 and 10 present a summary of peak and alternating stress data. Each measured (maximum and minimum) stress point was obtained by processing 10 stress cycles (10 revolutions for pinions, 10 planet passes for sun and ring gears) by computer program GSG. At 100 percent torque, up to six such data points were averaged together. At other torque values, only one measurement was made.

Peak Stress Results

Peak stress is plotted against gage location across the face width in figure 9. Peak stress results are summarized in table III. For comparison, the AGMA bending stress index number is also shown in table III for the combining pinions and for the ring gear. The index stress, based upon the Lewis equation for tooth bending stress, is typically much less than

TABLE III.—SUMMARY OF BENDING STRESS RESULTS
[Torque and speed at 100 percent]

	Peak stress		Mean stress		Alternating stress	
	MPa	(ksi)	MPa	(ksi)	MPa	(ksi)
Combining pinion						
Fillet gages	760	(110)	330	(48)	430	(62)
AGMA index	230	(33)	---	---	---	---
Root gages	260	(37)	40	(6)	220	(31)
Ring gear						
Fillet gages	410	(59)	60	(8)	340	(49)
AGMA index	330	(48)	---	---	---	---
Analytical	460	(67)	---	---	---	---
Root gages	320	(46)	−80	(−12)	400	(58)
Sun gear						
Root gages	−650	(−94)	−270	(−40)	380	(55)

that obtained from strain gages or calculated by finite-element methods. However, there is a large body of allowable stress data available in the AGMA standards which is consistent with the index stress procedure (ref. 17).

Figures 9(a) and (c) show maximum tensile fillet stresses in the combining pinions. Measured stress levels were consistently lower in the right than in the identical left pinion. The lower fillet stresses measured on the right pinion are believed to be due to improper gage placement on that gear. The maximum fillet stress is shifted towards the heel end of the gear, especially at higher torque levels. The greatest peak stress found is 760 MPa (110 ksi) on the left pinion. The left pinion peak stress is 230 percent greater than the AGMA index stress. Reference 13 reports other cases in which the measured stresses in spiral bevel gears were considerably greater than the AGMA index value.

Figures 9(b) and (d) compare peak root stress. Root stresses show much less variation across the face of the gear.

Maximum fillet tensile stress results for the ring gear at various gage locations are shown in figure 9(e). Bending stresses are slightly greater near the bottom of the ring gear than at the top. There is much less variation across the face width than on the spiral-bevel combining pinions and the stress distribution does not change with torque. The maximum fillet stress found is 410 MPa (59 ksi). This is 11 percent lower than the 460 MPa (67 ksi) obtained analytically. (See figure 7(d).) The measured stress is 24 percent greater than the AGMA index stress. Note that the AGMA method predicts that the ring gear will carry higher stresses than the combining pinion but the strain gage data show that the pinion is the more highly stressed gear.

Maximum compressive sun gear root stresses at various gage locations are plotted in figure 9(g). The maximum (compressive) stress found is −650 MPa (−94 ksi). The center gage (number 3) shows much lower stress levels than expected. This is believed to be caused by a defective or mismounted gage.

Alternating Stress Results

Alternating stress is plotted against torque level in figure 10. The alternating stress is calculated as one half of the algebraic difference between the maximum and minimum stress. All measurements show good linearity. The slopes of the lines connecting data points represent the torque dependence for the various gage locations. Alternating (and also mean) stress values are summarized in table III.

Figures 10(a) and (c) display alternating fillet stresses in the combining pinions. The gages near the toe end (numbers 1 and 2) show less torque dependence than those closer to the heel. The worst-case stress state found during this testing program was on the left combining pinion at 100 percent torque. Mean and alternating stress values at this location were 330 and 430 MPa (48 and 62 ksi). These mean and alternating stress values fall within the range of "successful test experience" reported in reference 14.

Alternating root stresses for the combining pinions are shown in figures 10(b) and (d). The root gages show less torque dependence and much less change in torque dependence between the gages.

Reference 18 reports strain gage testing on two of the gears of the Blackhawk Transmission. The stresses measured on the combining bevel pinion show the same general trend as those reported in reference 19 for the same gear but were about 50 percent lower in the root area. The root of the Sikorsky test pinion, however, was machined 0.5 mm (0.020 in.) undersized to accommodate the gages. This may account for the difference. The testing of reference 19 did not include fillet strain gages.

Figures 10(e) and (f) display fillet and root stresses in the ring gear. Sun gear alternating root stresses are shown in figure 10(g). These gages show less change in level and torque dependency between gages than for the spiral-bevel pinions.

The vibratory stress measured in the ring gear root of -80 ± 400 MPa (-12 ± 58 ksi) was about 70 percent higher than that reported in reference 19 at the same location. It is possible that differences in the gage length of the strain gages may account for this difference.

Summary of Results

The U.S. Army UH-60A (Black Hawk) helicopter transmission was tested at the NASA Lewis Research Center. Results obtained from these experimental strain-gage stress tests are as follows:

1. The largest stress measured was 760 MPa (110 ksi) on the fillet of the left spiral-bevel combining pinion. The corresponding mean and alternating stress values were 330 and 430 MPa (48 and 62 ksi). These values are within the range of successful test experience reported for other helicopter transmissions. The measured peak stress is 230 percent greater than the AGMA index stress.

2. On the ring gear fillet, the maximum stress was 410 MPa (59 ksi). Mean and alternating stresses were 60 and 340 MPa (8.7 and 49 ksi). The ring-gear peak fillet stress measured was

11 percent less than an analytical result of 460 MPa (67 ksi) and 24 percent greater than the AGMA index stress.

3. On the sun gear only root stresses were measured. The largest stress found was a compressive stress of −650 MPa (−94 ksi). Mean and alternating stresses were −270 MPa and 380 MPa (−39 and 55 ksi) respectively.

Lewis Research Center
National Aeronautics and Space Administration
Cleveland, Ohio, December 22, 1986

References

1. Cornell, R.W.: Compliance and Stress Sensitivity of Spur Gear Teeth. J. Mech. Des., vol. 103, no. 2, Apr. 1981, pp. 447—459.
2. Chang, S.H.; and Huston, R.L.: On Finite Element Stress Analysis of Spur Gears. NASA CR-167938, 1982.
3. Vijayakar, S.M.; and Houser, D.R.: The Use of Boundary Elements for the Determination of the Geometry Factor. AGMA Technical Paper 86-FTM-10, Oct. 1986.
4. Drago, R.J.; and Lutthans, R.V.: Combined Effects of Rim Thickness and Pitch Diameter on Spur Gear Tooth Stresses. American Helicopter Society Journal, vol 28, no. 3, July 1983, pp. 13-19.
5. Lin, H-H; and Huston, R.L.: Dynamic Loading on Parallel Shaft Gears. (UC-MIE-051586-19, Cincinnati Univ.; NASA Grant NSG-3188) CR-179473, 1986.
6. Hirt, M.C.O.: Stresses in Spur Gear Teeth and Their Strength as Influenced by Fillet Radius. (English Translation by J. Maddock), American Gear Manufacturers Assoc., 1976.
7. Boyd, L.S.; and Pike, J.: Multi-Mesh Gear Dynamics Program Evaluation and Enhancements. NASA CR-174747, 1985.
8. Pike, J.A.: Interactive Multiple Spur Gear Mesh Dynamic Load Program. NASA CR-165514, 1981.
9. Choy, F.K.; Townsend, D.P.; and Oswald, F.B.: Dynamic Analysis of Helicopter Multimesh Gear Transmissions. NASA TP-(to be published) 1987.
10. August, R.; et al.: Dynamics of Planetary Gear Trains. NASA CR-3793, 1984.
11. Winter, H.; and Paul, M.: Influence of Relative Displacements Between Pinion and Gear on Tooth Root Stresses of Spiral Bevel Gears. J. Mech. Transmissions Automated Design, vol. 107, no. 1, Mar. 1985, pp. 43-48.
12. Mack, J.C.; and McCann, R.F.: Testing Large Transmissions. National Specialists' Meeting on Helicopter Test Technology, American Helicopter Society, 1984.
13. Albrecht, C.: Developments in Gear Analysis and Test Techniques for Helicopter Drive Systems. ASME Paper 79-DE-15, May 1979.
14. Weiss, W.; Walsh, G.; and Mack, J.: Heavy Lift Helicopter Forward Transmission Program. USAAVSCOM TR-85-D-19, May 1986.
15. Mitchell, A.M.; Oswald, F.B.; and Coe, H.H.: Testing of UH-60A Helicopter Transmission in NASA-Lewis 2240-kW (3000-hp) Facility. NASA TP-2626, 1986.
16. Mitchell, A.M.; Oswald, F.B.; and Schuller, F.T.: Testing of YUH-61A Helicopter Transmission in NASA-Lewis 2240-kW (3000-hp) Facility. NASA TP-2538, 1986.
17. Coy, J.J.; Townsend, D.P.; and Zaretsky, E.V.: Gearing. NASA RP-1152, 1985.
18. Haven, R.: Transmission, Main, Baseline Operating Data Survey Report. SER-70419, Sikorsky Aircraft Co., 1981.

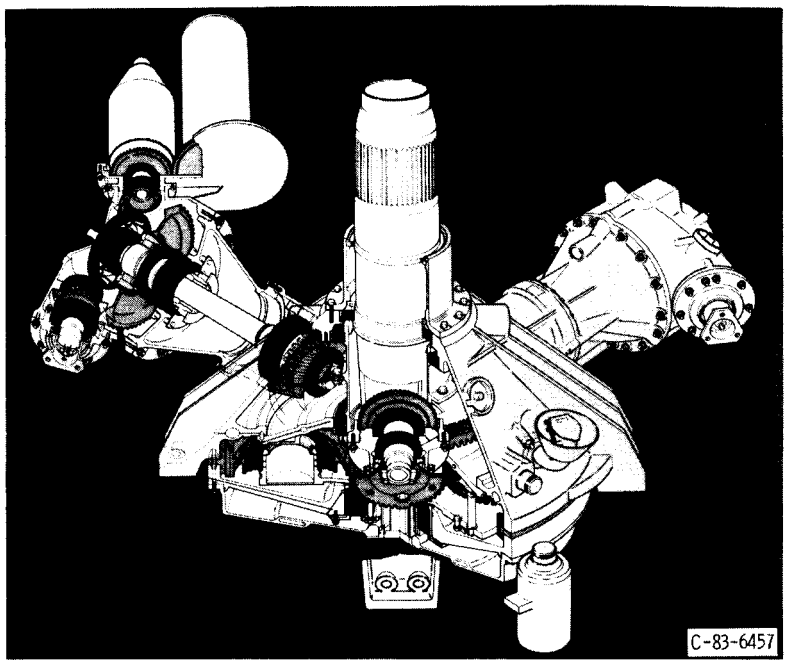

Figure 1.—Isometric view of UH60A helicopter transmission.

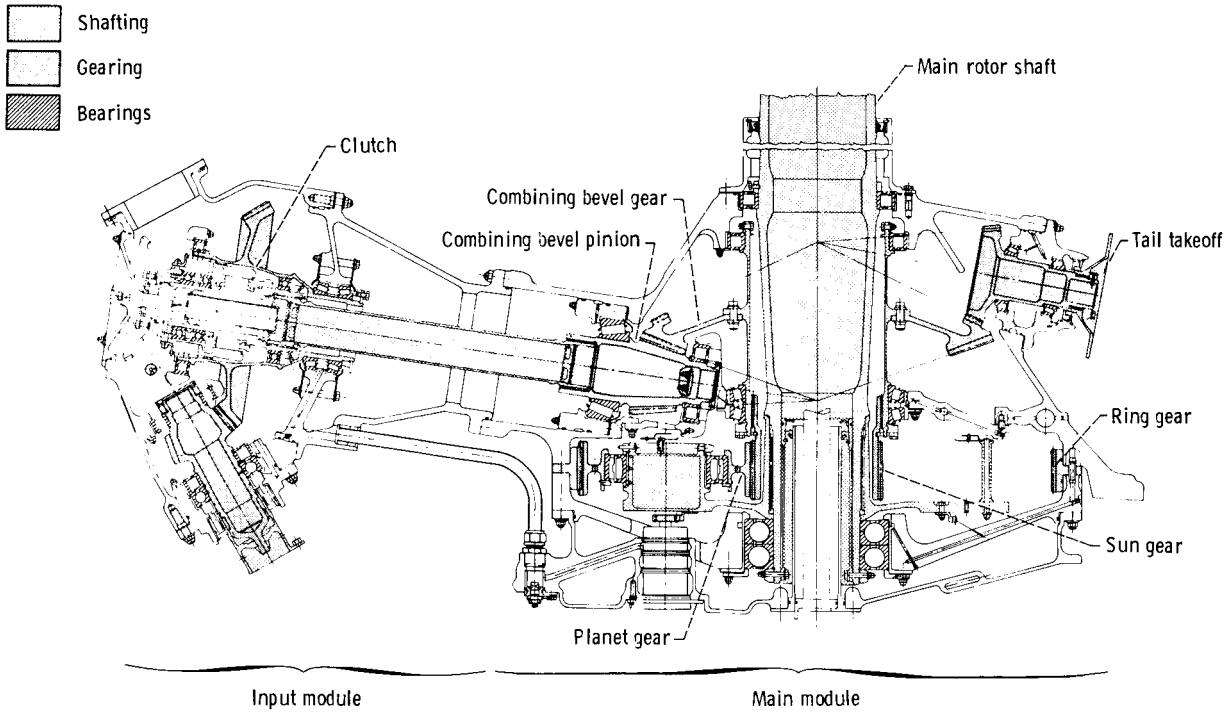

Figure 2.—Section view along input module and tail of UH60A helicopter transmission.

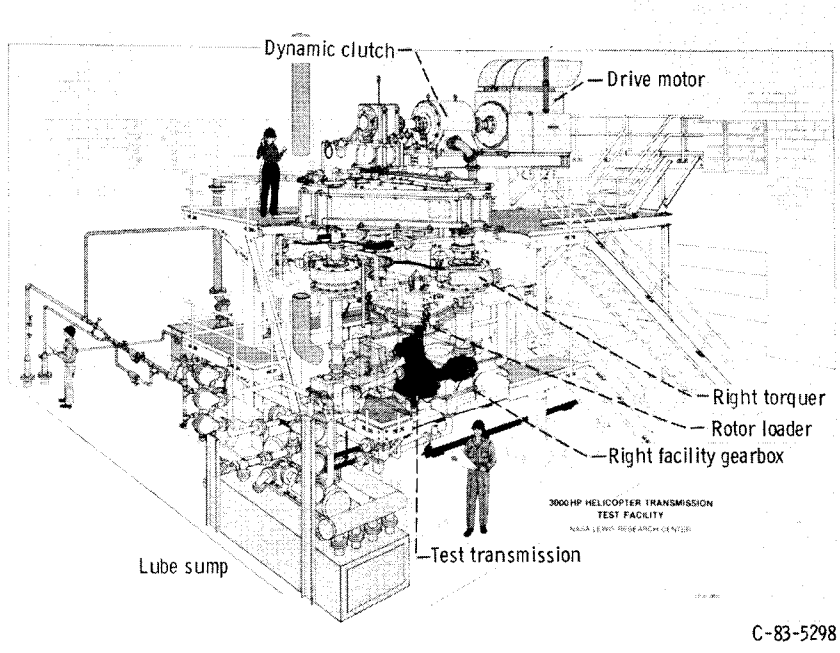

Figure 3.—NASA Lewis Helicopter Transmission Test Facility.

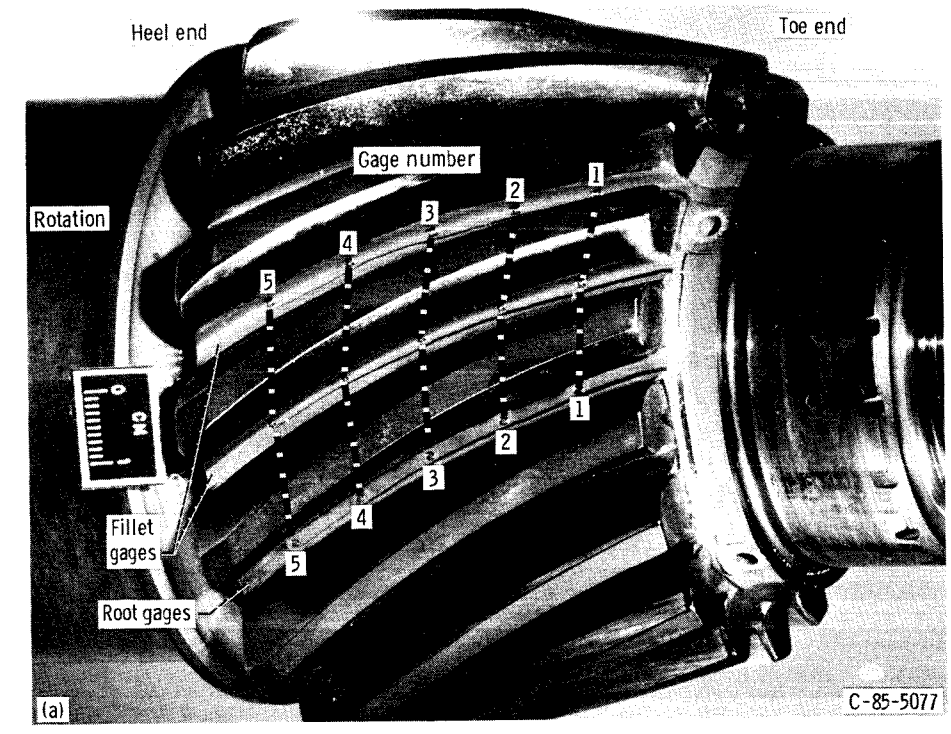

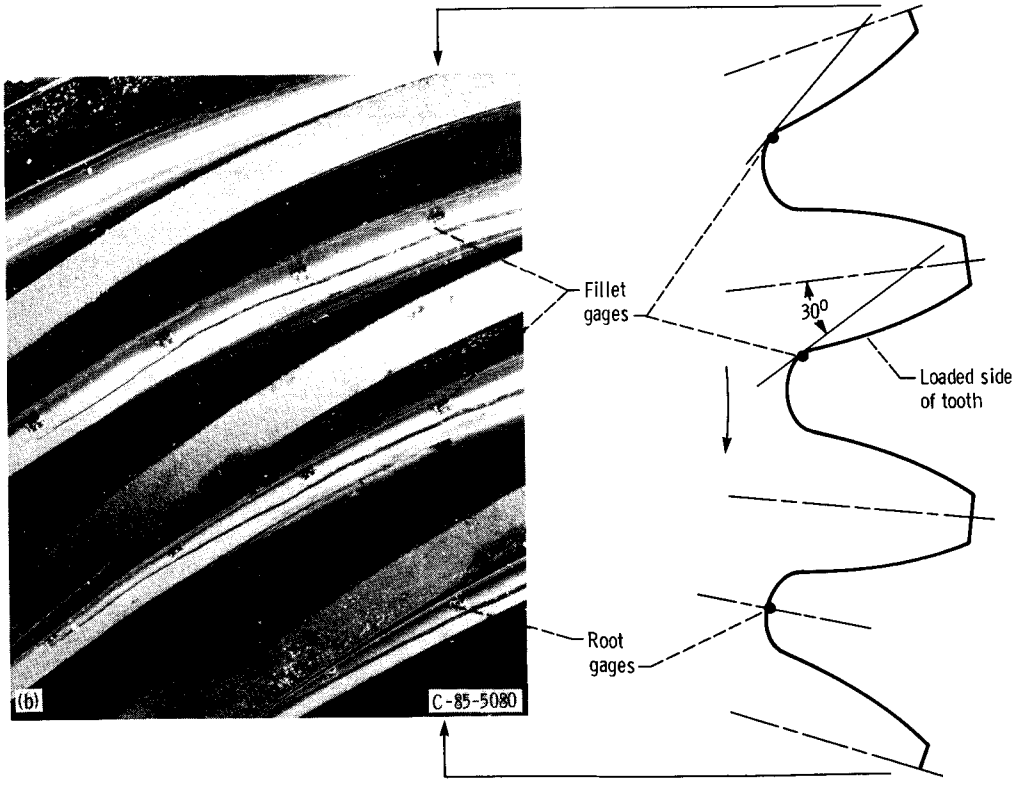

(a) Pinion showing gage locations.
(b) Detail of pinion.

Figure 4.—Strain gage installation on spiral-bevel combining pinions.

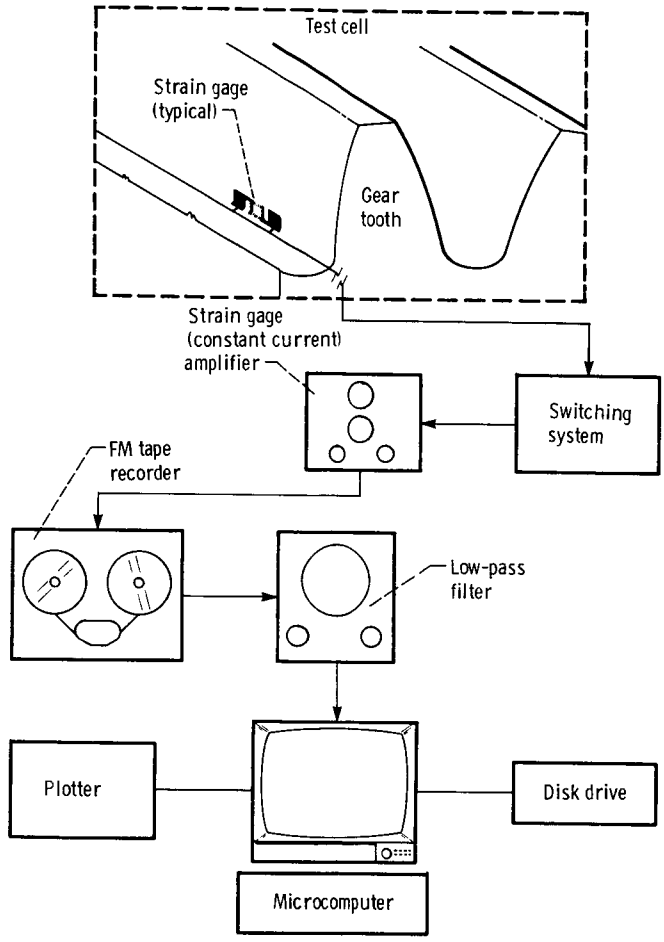

Figure 5.—Stress-strain measurement system.

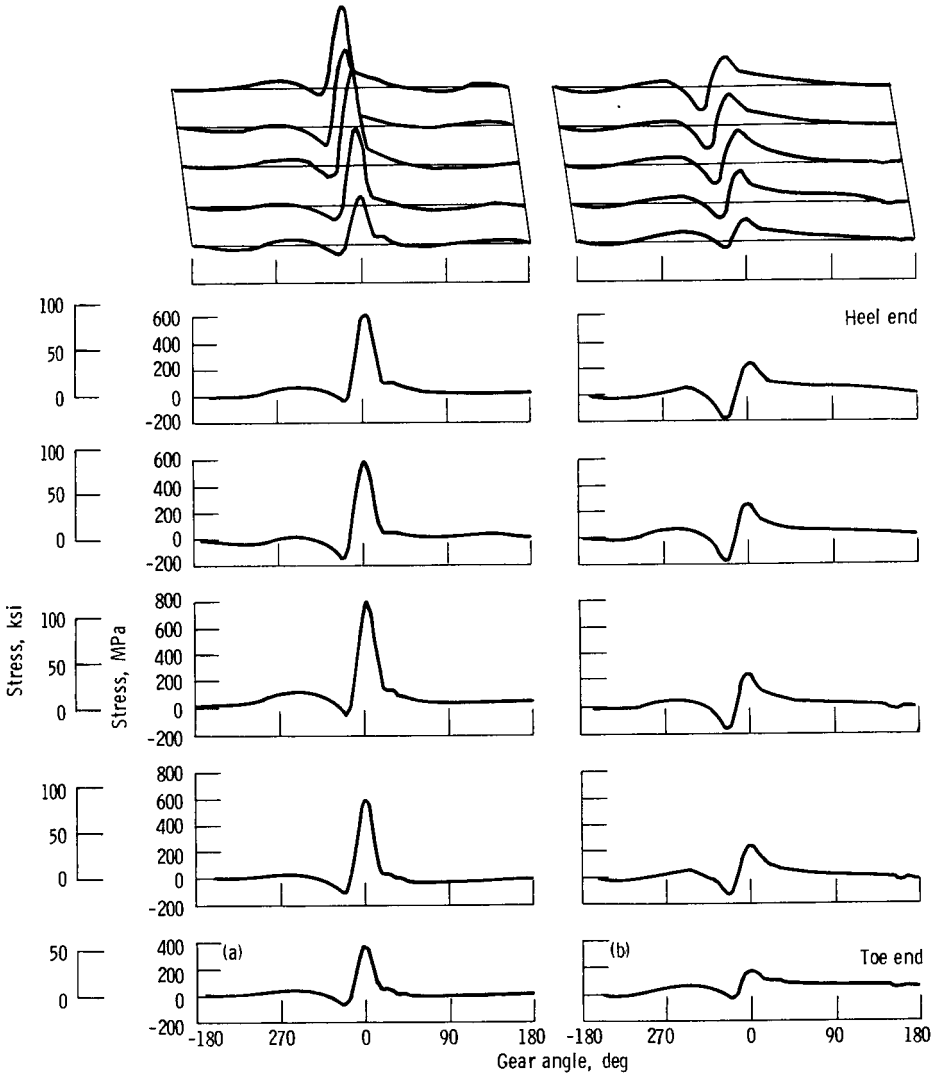

(a) Fillet gages.
(b) Root gages.

Figure 6.—Typical stress traces for one revolution of spiral-bevel combining pinion.

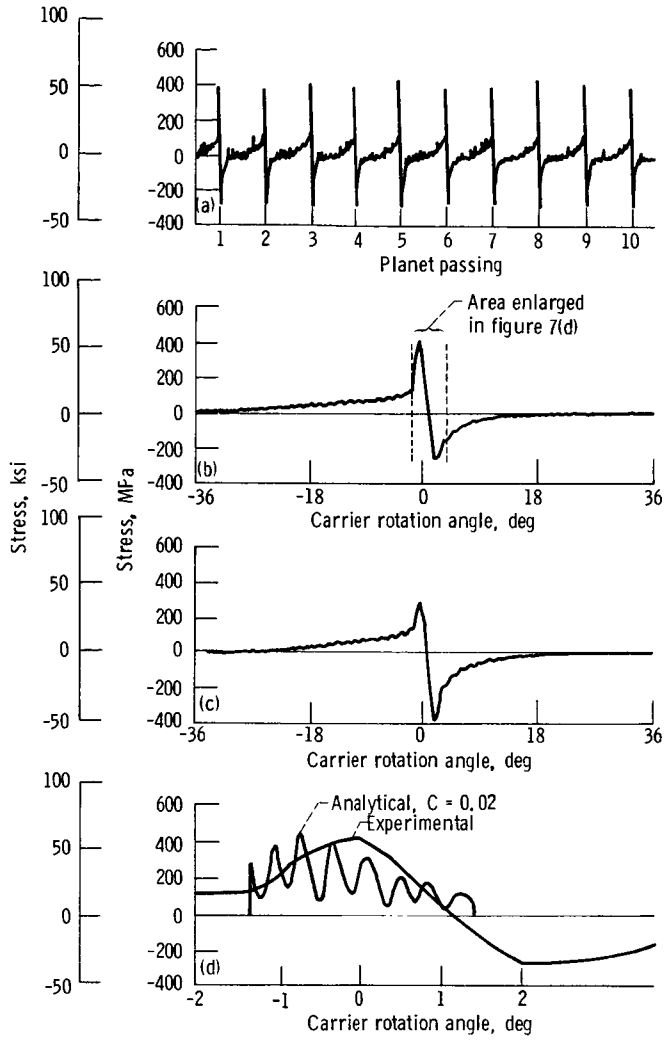

(a) Fillet gages (showing 10 planet passes).
(b) Fillet gage cycle (averaged from 10 planet passes).
(c) Root gage cycle (averaged from 10 planet passes).
(d) Comparison of analytical and experimental results for one tooth mesh.

Figure 7.—Stress in ring gear.

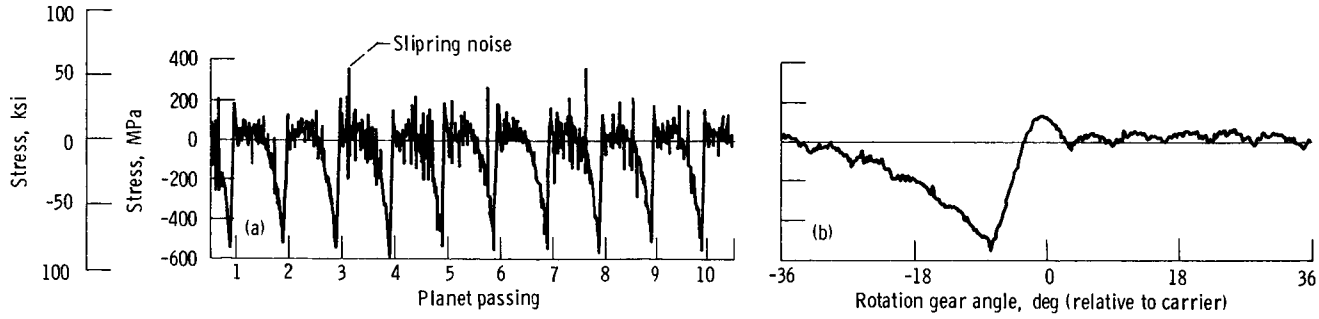

(a) Root gages (showing 10 planet passes).
(b) Root gage cycle (averaged from 10 planet passes).

Figure 8.—Stress in sun gear.

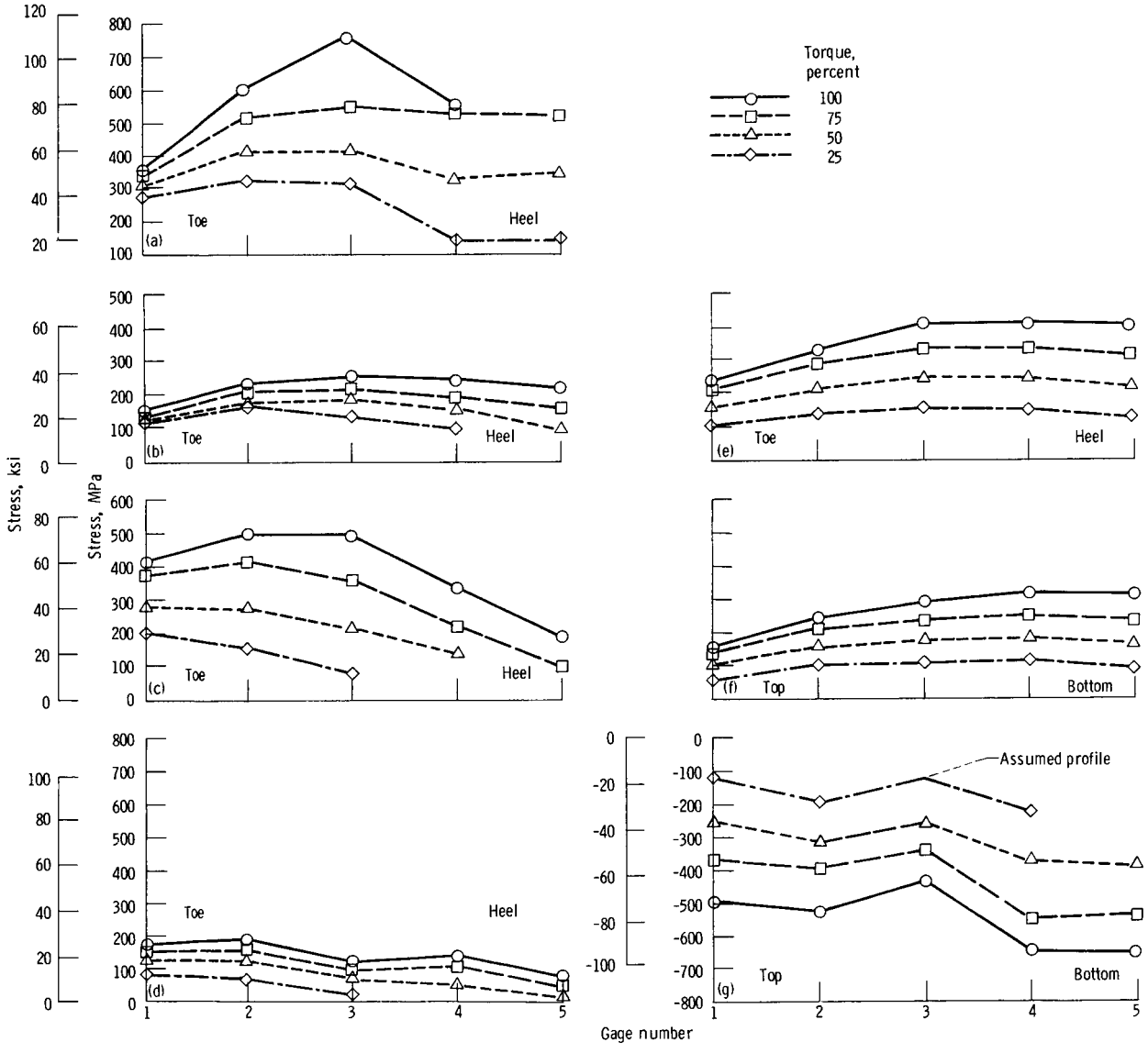

(a) Left combining pinion, fillet gages.
(b) Left combining pinion, root gages.
(c) Right combining pinion, fillet gages.
(d) Right combining pinion, root gages.
(e) Ring gear, fillet gages.
(f) Ring gear, root gages.
(g) Sun gear, root gages (compressive stress shown).

Figure 9.—Peak (maximum) tensile stress as compared to gage location (at four torque levels).

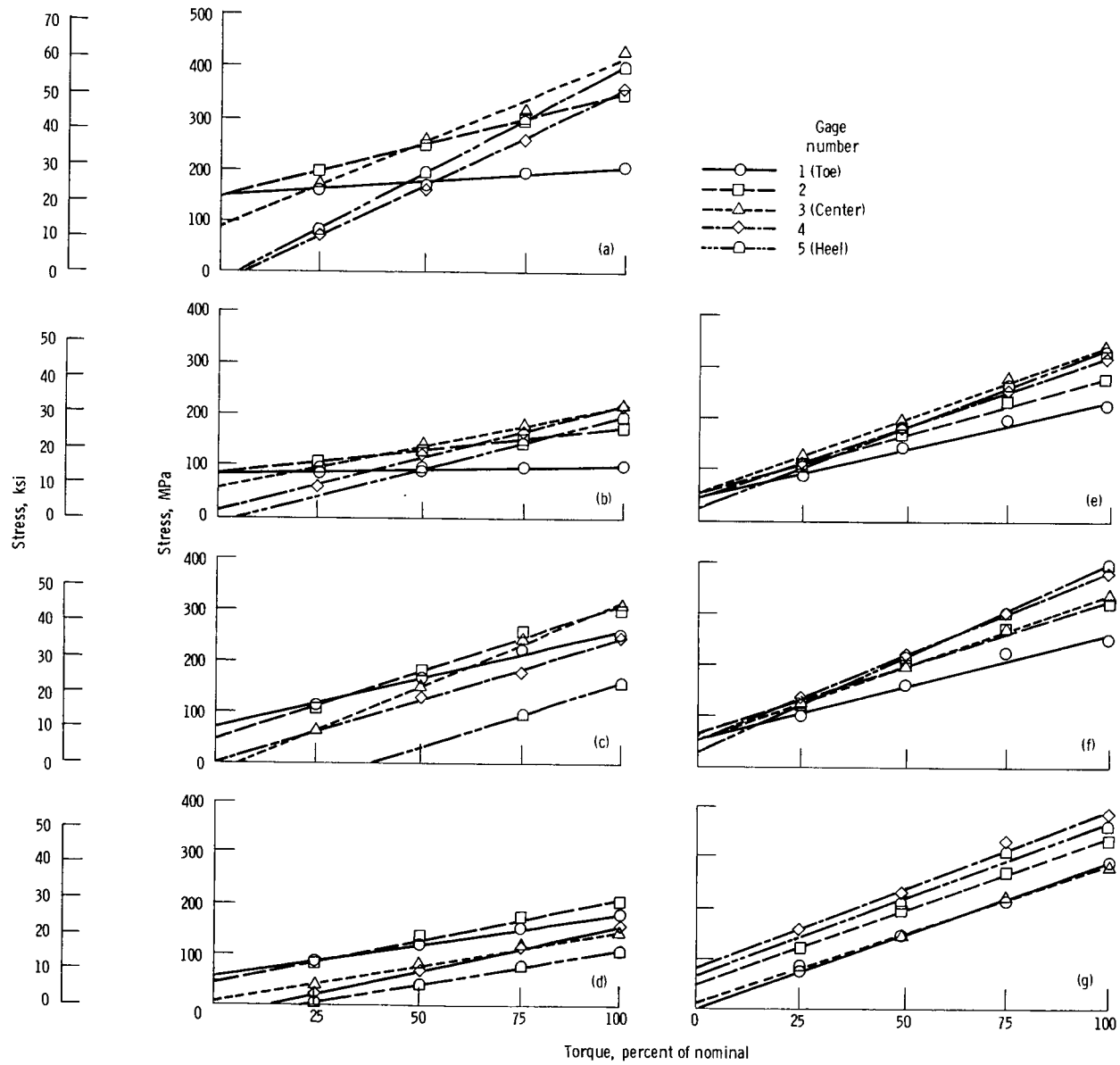

(a) Left combining pinion, fillet gages.
(b) Left combining pinion, root gages.
(c) Right combining pinion, fillet gages.
(d) Right combining pinion, root gages.
(e) Ring gear, fillet gages.
(f) Ring gear, root gages.
(g) Sun gear, root gages.

Figure 10.—Alternating stress as compared to transmission torque.

1. Report No.	2. Government Accession No.	3. Recipient's Catalog No.
NASA TP-2698		

4. Title and Subtitle	5. Report Date
Gear Tooth Stress Measurements on the UH-60A Helicopter Transmission	March 1987
	6. Performing Organization Code: 505-63-51
7. Author(s): Fred B. Oswald	8. Performing Organization Report No.: E-3357
	10. Work Unit No.
9. Performing Organization Name and Address: National Aeronautics and Space Administration, Lewis Research Center, Cleveland, Ohio 44135	11. Contract or Grant No.
	13. Type of Report and Period Covered: Technical Paper
12. Sponsoring Agency Name and Address: National Aeronautics and Space Administration, Washington, D.C. 20546	14. Sponsoring Agency Code

15. Supplementary Notes

16. Abstract

The U.S. Army UH-60A (Black Hawk) 2200-kW (3000-hp) class twin-engine helicopter transmission was tested at the NASA Lewis Research Center. Results from these experimental (strain-gage) stress tests will enhance the data base for gear stress levels in transmissions of a similar power level. Strain-gage measurements were performed on the transmission's spiral-bevel combining pinions, the planetary sun gear, and ring gear. Tests were performed at rated speed and at torque levels 25 to 100 percent that of rated. One measurement series was also taken at a 90 percent speed level. The largest stress found was 760 MPa (110 ksi) on the combining pinion fillet. This is 230 percent greater than the AGMA index stress. Corresponding mean and alternating stresses were 330 and 430 MPa (48 and 62 ksi). These values are within the range of successful test experience reported for other transmissions. On the fillet of the ring gear, the largest stress found was 410 MPa (59 ksi). The ring-gear peak stress was found to be 11 percent less than an analytical (computer simulation) value and it is 24 percent greater than the AGMA index stress. A peak compressive stress of 650 MPa (94 ksi) was found at the center of the tooth root of the sun gear.

17. Key Words (Suggested by Author(s))	18. Distribution Statement
Strain-gage testing; Helicopter; Transmission; Spiral-bevel gears; Planetary gears	Unclassified – unlimited STAR Category 37

19. Security Classif. (of this report)	20. Security Classif. (of this page)	21. No of pages	22. Price*
Unclassified	Unclassified	15	A02

*For sale by the National Technical Information Service, Springfield, Virginia 22161

NASA-Langley, 1987